Available online at www.sciencedirect.com
ScienceDirect
Acta Materialia 54 (2006) 5221–5229
Acta MATERIALIA
www.actamat-journals.com

Effects of frequency, composition, hydrogen and twin boundary density on the internal friction of $Ti_{50}Ni_{50-x}Cu_x$ shape memory alloys

G. Fan [a,b], Y. Zhou [a,b], K. Otsuka [a,c,*], X. Ren [a,b], K. Nakamura [a], T. Ohba [d], T. Suzuki [a], I. Yoshida [e], F. Yin [a]

[a] Ferroic Physics Group, National Institute for Materials Science, 1-2-1 Sengen, Tsukuba 305-0047, Japan
[b] Multi-disciplinary Materials Research Centre and State Key Laboratory for Mechanical Behaviour of Materials, Xi'an Jiaotong University,Xi'an 710049, China
[c] Foundation for Advancement of International Science, Akatsuka, Aza-ushigahuchi, Tsukuba 305-0062, Japan
[d] Department of Materials Science, Shimane University, Nishikawatsu, Matsue 690-8504, Japan
[e] Department of Science and Engineering, Iwaki Meisei University, Iwaki 970-8551, Japan

Received 19 February 2006; received in revised form 15 May 2006; accepted 12 June 2006
Available online 18 September 2006

Abstract

The internal friction (IF) of $Ti_{50}Ni_{50-x}Cu_x$ polycrystals, which were normally solution-treated, was systematically studied using dynamic mechanical analysis. As a result, the broad peak appearing in B19 martensite was confirmed to be a relaxation peak with an activation energy of 0.67 and 0.76 eV for $x = 20$ and 16, respectively. Then the broad peak was shown to disappear in a single-crystal experiment, if twin boundaries in martensite are largely eliminated. This is direct evidence to show twin boundaries are indispensable for the broad peak. The effect of hydrogen on IF was also examined using a vacuum system with a mass spectrometer, and the broad peak at 250 K was observed to disappear, while a new small relaxation peak was found at 178 K, when hydrogen was eliminated. These experiments clearly show that there are two essential ingredients to observe the high broad peak: twin boundaries and hydrogen. Based on these results a possible origin for the broad peak is discussed.

Keywords: Dynamic mechanical analysis; Internal friction; Shape memory alloys; Relaxation; Twin boundary

1. Introduction

The needs for high-damping materials with high strength are increasing to reduce vibrations and noises in buildings and transportation vehicles, etc., in the modern world. As such materials, shape memory alloys in the martensitic state are attracting much attention, because they a contain a high density of twins as a lattice invariant strain upon martensitic transformation [1,2]. In particular, Ti–Ni alloys are important in this respect, since their mechanical properties are superior compared to other shape memory alloys [3,4]. However, one of the shortcomings of Ti–Ni alloys is that the transformation temperatures are not particularly high, usually around room temperature or less. However, it is possible to increase the transformation temperatures by substituting Ni with substantial amounts of Cu [5]. Thus Ti–Ni–Cu alloys are interesting from the viewpoint of developing high-damping materials, which may be used at temperatures even above room temperature.

$Ti_{50}Ni_{50-x}Cu_x$ alloys are rather unique in their martensitic transformation behavior [3–12]. They exhibit the B2–B19 (orthorhombic)–B19′ (monoclinic) two-stage transformation for the composition $x \geqslant 5$ [5]. However, the second B19–B19′ transformation was found to be very sluggish and the fraction transformed to be very small even at 90 K [12]. The internal friction (IF) of the alloy system was studied by various researchers [2,13–15,17–21], and

* Corresponding author. Address: Ferroic Physics Group, National Institute for Materials Science, 1-2-1 Sengen, Tsukuba 305-0047, Japan. Tel.: +81 29 859 2707; fax: +81 29 859 2701.
E-mail address: otsuka.kazuhiro@nims.go.jp (K. Otsuka).

1359-6454/$30.00
doi:10.1016/j.actamat.2006.06.018

the following two peaks are known: (1) B2–B19 transformation peak (often called the "transient peak", because the peak diminishes greatly when temperature is fixed) [2] and (2) the "broad peak" situated around 250 K for the present alloy system, which does not diminish even when temperature is fixed [2]. Of these two, the broad peak is important from the viewpoint of practical applications, since it does not diminish even at a fixed temperature. Also, it was recently shown that $Ti_{50}Ni_{50-x}Cu_x$ alloys with $x = 20$ and 16 exhibit extremely high IF, e.g. $Q^{-1} = 0.2$ from the low-frequency torsion pendulum method [2]. The broad peak is also found in Ti–Ni binary alloys at about 200 K and is believed to be of relaxation-type [16,22–24]. The broad peak in Ti–Ni–Cu alloys was also reported to be the relaxation-type [17,18,21]. However, the origin of the relaxation peak is still controversial. Yoshida et al. [2] proposed that it originates from twin boundary motion, which exists with high density in martensite, and explained that the extremely high IF in $Ti_{50}Ni_{50-x}Cu_x$ alloys is due to the very high mobile nature of the twin boundaries in the martensite, because the associated twinning shears in B19 martensite are very small compared with those in B19′ martensite. Mazzolai's group [16–19] extensively studied the IF in Ti–Ni-based alloys including Ti–Ni–Cu, especially as regards the effect of hydrogen, and attributed the broad peaks in Ti–Ni-based alloys to hydrogen relaxation or to the stress-induced diffusion of hydrogen [19], although they also suggested a twin boundary effect called P_{TWM} [16] and hydrogen–twin boundary complex effect in other papers [17,18]. However, the peak they observed in a pre-strained and aged Ti–Ni alloy [16] is a non-thermally activated peak, which is not the main theme of the present paper. Sakaguchi et al. [21] studied $Ti_{50}Ni_{25}Cu_{25}$ alloy, which was made by the Ti–Ni/Cu laminated method, and also followed the interpretation of the hydrogen effect, and suggested the IF peak as due to the Snoek–Koester effect [25,26], which originates from the interaction of hydrogen with dislocations. Meanwhile, the present authors had a different view in initiating the present work, because the broad peak appears even when careful experiments are carried out in which hydrogen is excluded in an ordinary sense. Moreover, it has been noted that the broad peak appears also in other shape memory alloys with high density of twin boundaries, such as Mn–Cu [27,28], Au–Cd [29], and Cu–Zn–Al–Ni [30,31], etc., which do not appear to be hydrogen-absorbing materials, in contrast to Ti–Ni, in which Ti is a hydrogen-absorbing material. Thus the view was taken that the broad peak is due to the intrinsic back and forth twin boundary motion under stress rather than to the relaxation based on the diffusion of hydrogen.

Thus the present work reports a systematic study of the IF of $Ti_{50}Ni_{50-x}Cu_x$ ($x = 10, 16, 20$) alloys for both polycrystals and single crystals to understand the nature of the broad peak and other peaks. We employed dynamic mechanical analysis (DMA) to measure IF and storage modulus. Using this method we can easily determine the frequency-related properties, since a specimen can be measured with various frequencies in a single test. We emphasize here that most of the experiments were carried out for specimens that were heat-treated in a system without introducing hydrogen in the ordinary sense, as explained in detail in the next section. In addition, to check the effect of hydrogen we used another system, in which hydrogen can be easily eliminated and/or added.

2. Experimental

Alloys with nominal composition $Ti_{50}Ni_{50-x}Cu_x$ ($x = 10, 16, 20$) were prepared as described previously [2]. The specimens used in the experiments were solution-treated at 1273 K for 1.5 h in quartz tubes filled with Ar gas and Ti-getter to avoid oxidation. This was followed by water quenching by breaking the tubes and chemical etching to remove the oxidized surface layer. The specimens were subjected to chemical analysis using ICP-OES emission spectrometry, and the results are shown in Table 1. Although there are some deviations from the nominal compositions, we will use the nominal compositions to specify the alloys for simplicity in the following. The transformation temperatures measured using differential scanning calorimetry (DSC) and electrical resistivity are also shown in Table 1. The IF and storage modulus were measured using DMA (Q800 from TA Co.). Specimens with a size of $50 \times 1.5 \times 1.5\ mm^3$ were measured at a constant amplitude of 15 μm (the corresponding strain amplitude was 2×10^{-4}) in dual cantilever mode, unless otherwise specified. The temperature was changed from 393 to 133 K step by step (termed step-cooling or step-heating hereafter), i.e. specimens were kept isothermally for 5 min at every testing temperature to reach an equilibrium state. We employed this step-cooling/heating method mostly in order to quantify the features of the broad peak, such as frequency dependence and temperature hysteresis, although continuous cooling/heating was sometimes used for efficient measurements. Transformation peaks become very weak or disappear due to the zero cooling rate in the former measurements. This also benefits our study for the broad peak. The IF $\tan\delta$ and storage

Table 1
Specimen composition and transformation temperatures

Nominal composition	Results of chemical analysis	O_s (B2–B19) (K)	AO_s (B19–B2) (K)	M_s[a] (B19–B19′) (K)	A_s (B19′–B19) (K)
$Ti_{50}Ni_{30}Cu_{20}$	$Ti_{47.4}Ni_{31.7}Cu_{20.9}$	348	344	192	–
$Ti_{50}Ni_{34}Cu_{16}$	$Ti_{45.6}Ni_{37.6}Cu_{16.8}$	349	334	273	–
$Ti_{50}Ni_{40}Cu_{10}$	$Ti_{50.5}Ni_{39.9}Cu_{9.6}$	331	321	298	–

[a] M_s for B19–B19′ transformation taken from Refs. [11,12].

modulus were automatically recorded when the frequency was changed from 0.2 to 20 Hz discretely at each equilibrium temperature. The hydrogen content of the specimens was measured by chemical analysis (by the inert gas fusion method) after DMA measurements, as described below.

To study the effect of hydrogen, we used a vacuum system equipped with a quadrupole mass spectrometer, evacuated using a turbomolecular pump. Thus, we could identify gas species such as H_2^+ upon dehydrogenation. Specimens were heated to 1173 K in a furnace in a dynamic vacuum state, which was continuously evacuated. This is the dehydrogenation process in which hydrogen atoms can be removed from the specimen due to its low solubility at high temperature. Then the specimens were cooled to room temperature by rapidly removing them from the furnace, but still kept in quartz tubes to avoid oxidation. Specimens after dehydrogenation (DeH) were measured using DMA again with the same method. To further confirm the effect of hydrogen, a small amount of hydrogen was doped into the specimens by keeping them in a H_2-containing closed quartz tube. The results for normally heat-treated specimens, DeH ones and hydrogen-doped ones are discussed in the next section. The experiments described above were carried out with polycrystal specimens. However, we also used a $Ti_{50}Ni_{30}Cu_{20}$ single crystal, made by the Bridgman method, in an experiment to study the important role of twin boundaries in martensites, as discussed later.

3. Results and discussion

3.1. Frequency dependence of IF

In the following we discuss the results for $Ti_{50}Ni_{30}Cu_{20}$ alloy first, since it was most extensively studied, and the results are rather straightforward compared to others. Fig. 1(a) shows $\tan\delta$ and storage modulus vs. temperature curves upon cooling under various frequencies for the specimen annealed at 1273 K for 1.5 h followed by quenching into water. Here δ is the phase difference between applied stress and the resulting strain, and thus $\tan\delta$ represents IF, which is equal to Q^{-1}. The data were taken under step-cooling conditions, as described in Section 2. From this figure we see two peaks. From high-temperature side, the first one, accompanying a sharp decrease in storage modulus, corresponds to the transient peak for B2–B19 transformation, the start temperature of which agrees well with temperature O_s measured by DSC, as indicated. At lower temperature we see the second peak with $\tan\delta$ as high as 0.12. This is the so-called broad peak. We can see the peak position has a strong frequency dependence. Furthermore we note that the curvature of the storage modulus changes sign at the temperature that roughly corresponds to the peak temperature of the broad peak. In a previous paper [11] we reported, from synchrotron radiation experiments, that this peak (shown in the corresponding Fig. 5 in Ref. [2]) is a broad peak due to the twin boundary motion

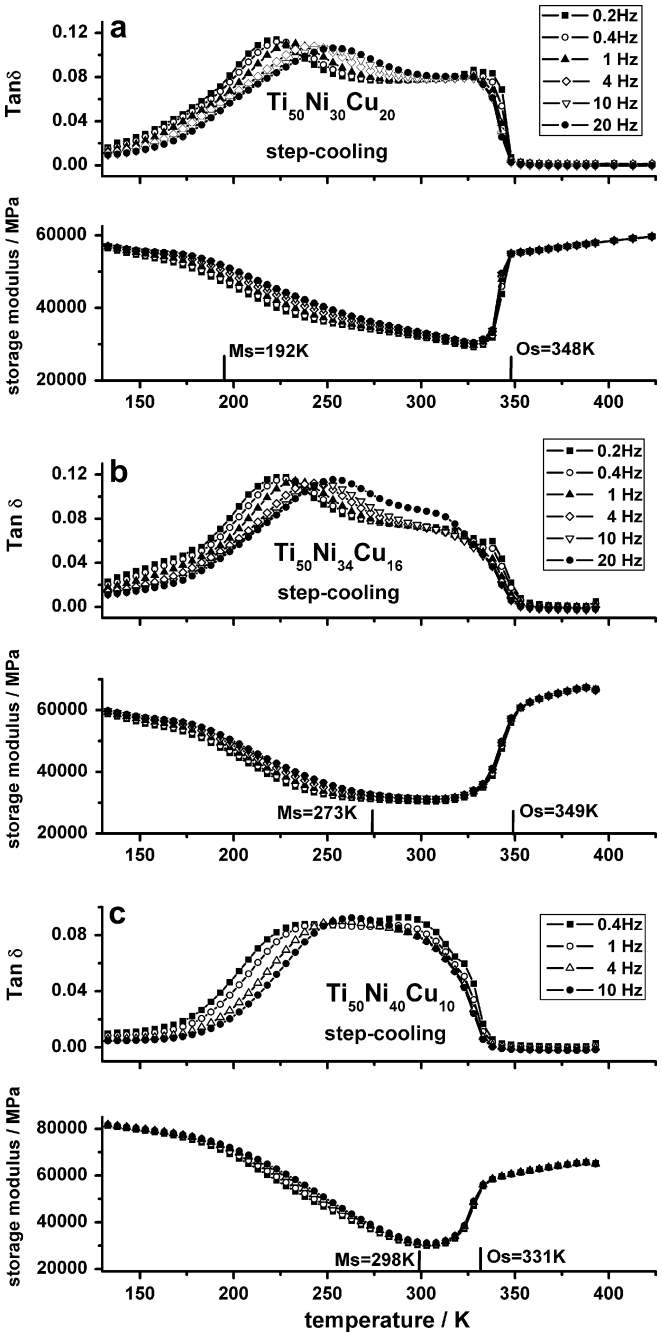

Fig. 1. IF $\tan\delta$ and storage modulus as a function of temperature during step-cooling in DMA multi-frequency strain test mode: (a) $Ti_{50}Ni_{30}Cu_{20}$, (b) $Ti_{50}Ni_{34}Cu_{16}$, (c) $Ti_{50}Ni_{40}Cu_{10}$ alloys. Different symbols represent different frequency as indicated. O_s and M_s indicated above the horizontal axis represent the transformation start temperatures upon cooling for B2 → B19 and B19 → B19′ transformations, respectively. O_s was determined by DSC and M_s was determined by in situ X-ray diffraction coupled with electrical resistivity measurement [11,12]. Specimens were solution-treated at 1273 K for 1.5 h, followed by water quenching. See text for details.

in B19 martensite rather than a transient peak for the second B19–B19′ transformation, because M_s (= 192 K) for this transformation is much lower for the composition of this alloy. The frequency dependence feature of the peak positions described above strongly suggests that the broad

peak is a relaxation-type [32]. For a relaxation process, the peak temperature T_p is determined from the following equation:

$$\omega\tau = 2\pi f\tau_0 \exp(E/k_B T_p) = 1 \quad (1)$$

where ω is angular frequency, τ relaxation time, f the frequency, E the activation energy for the relaxation process and k_B the Boltzmann constant. Thus the natural logarithm of frequency in Fig. 1(a) is plotted as a function of $1/T$, and the fitted straight line was determined by the least squares method (Fig. 2(a)). We see a good linear fit between ln f and $1/T$ for the broad peaks in Fig. 1(a). This also supports the assertion that the broad peak is a relaxation-type. From the slope of the fitted line and the extrapolation of $1/T$ to zero, the activation energy and the relaxation time τ_0 were determined as follows: $E = 0.67 \pm 0.01$ eV, $\tau_0 = 2.0 \times 10^{-15\pm0.1}$ s. This was a result of linear fitting for the data upon step-cooling. Interestingly, if we make a similar fitting for the data upon step-heating, we found a slightly different result: $E = 0.64 \pm 0.01$ eV, $\tau_0 = 1.4 \times 10^{-14\pm0.2}$ s. The origin of such a difference arises from the presence of a small temperature hysteresis upon cooling and heating, as discussed later with respect to Fig. 3. We

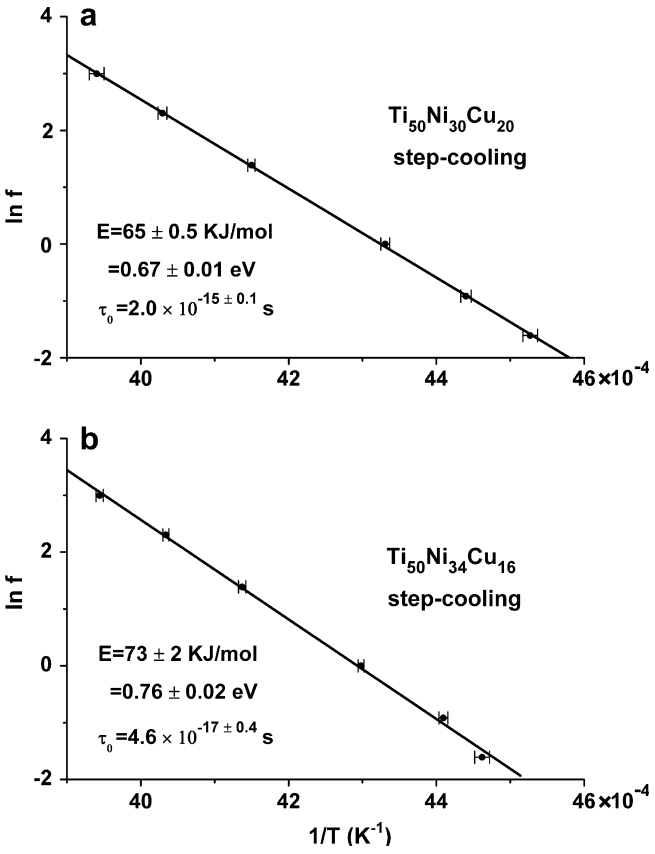

Fig. 2. Natural logarithm of frequency (f) plotted as a function of the reciprocal peak temperature ($1/T$) according to the broad peak in Fig. 1(a) and (b), and the fitted straight line determined by the least squares method. E and τ_0 represent the activation energy and the relaxation time, respectively. The error bars represent the uncertainty in determining the peak temperature.

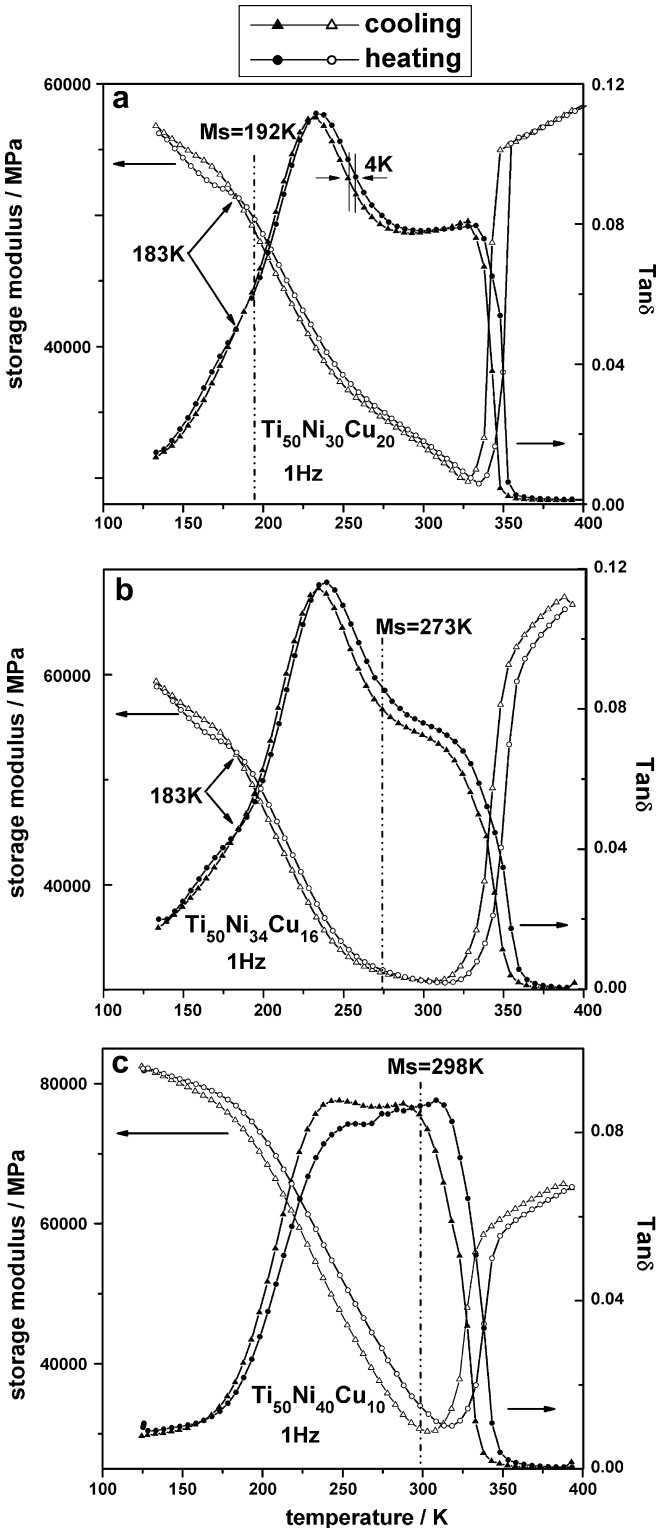

Fig. 3. Storage modulus (open symbols) and tan δ (filled symbols) shown as a function of temperature during both step-cooling and step-heating with a frequency of 1 Hz: (a) $Ti_{50}Ni_{30}Cu_{20}$, (b) $Ti_{50}Ni_{34}Cu_{16}$, (c) $Ti_{50}Ni_{40}Cu_{10}$. The dash-dotted lines indicate the M_s temperature for the B19–B19′ martensitic transformation determined by in situ X-ray diffraction coupled with electrical resistivity measurements [11,12]. Specimens were solution-treated at 1273 K for 1.5 h, followed by water quenching.

will discuss the meaning of the relaxation process after we have discussed the effect of hydrogen on the IF.

The behavior of $\tan\delta$ and storage modulus as a function of temperature for $Ti_{50}Ni_{34}Cu_{16}$ alloy is similar to the above case, as shown in Fig. 1(b), and thus the description will be brief. In this case the transformation start temperature for the B19–B19′ transformation ($M_s = 273$ K) comes above the peak temperature of the broad peak. Thus the broad peak and transient peak due to the second transformation overlap. However, the second transformation for this composition is very sluggish and the fraction transformed is very small, as described previously [11,12]. Thus the effect of the second transformation on the broad peak is rather small, and consequently the frequency-dependent broad peak looks similar to that of $Ti_{50}Ni_{30}Cu_{20}$, as shown in Fig. 1(a). The relationship between the peak temperature and frequency upon cooling is shown in Fig. 2(b), from which the activation energy and the relaxation time were determined to be $E = 0.76 \pm 0.02$ eV, $\tau_0 = 4.6 \times 10^{-17\pm0.4}$ s. The similar values upon heating were $E = 0.71 \pm 0.02$ eV, $\tau_0 = 6.4 \times 10^{-16\pm0.6}$ s. These will be discussed later together with the previous case.

The behavior of $\tan\delta$ and storage modulus as a function of temperature for $Ti_{50}Ni_{40}Cu_{10}$ alloy is shown in Fig. 1(c). The broad peak in this case is not well developed, although the frequency-dependent features still can be seen in both the $\tan\delta$ and storage modulus curves in the temperature range of the broad peak. This is because of the high M_s value ($M_s = 298$ K) of this alloy. The overlapping of the broad peak and that of the second transformation becomes marked. A much larger fraction of B19 has transformed into B19′ in the temperature range of the broad peak compared with the previous two cases. Thus the $\tan\delta$ value is smaller than the previous two cases. The linear fitting of frequency against the peak temperature ($1/T$) was not carried out for this case.

3.2. The third IF peak and hysteresis of the broad peak

Although not clear in Fig. 1, there is a third peak, which becomes clear by showing cooling and heating curves together. Fig. 3(a) shows such curves for $Ti_{50}Ni_{30}Cu_{20}$ alloy under 1 Hz for both step-cooling and step-heating. We notice this very small peak from hysteresis loops both in IF and storage modulus curves in the temperature range between 183 and 145 K. The presence of a hysteresis loop strongly suggests that it is due to some kind of transformation, possibly a martensitic transformation, because it occurs at such a low temperature. It would be easy to attribute it to the second B19–B19′ transformation, because M_s for the $Ti_{50}Ni_{30}Ci_{20}$ alloy ($M_s = 192$ K) is close to the temperature where the hysteresis loop appears. However, the similar third peak appears at a similar temperature for $Ti_{50}Ni_{34}Cu_{16}$ alloy as well (see Fig. 3(b)), although M_s for the second transformation is much higher in this case ($M_s = 273$ K). Also, the third peak does not appear for $Ti_{50}Ni_{40}Cu_{10}$ alloy (see Fig. 3(c)). Thus it is not possible to ascribe the third peak to the second B19–B19′ transformation. At present the authors think that it may be due to a martensitic transformation of precipitates. It is known in Ni-rich binary alloys that the precipitate Ti_2Ni_3 also transforms martensitically a little above room temperature [33]. In the case of the present alloy system the precipitate is not of Ti_2Ni_3 type but of Ti_2(Ni,Cu) type [15,34], and it is not confirmed yet whether the latter also transforms martensitically or not. However, the presence of the hysteresis is most easily understood by such a proposition. Besides, the following considerations also support this view. In the ternary Ti–Ni–Cu alloys the precipitates are most likely to appear when the Ti content is off the stoichiometry of 50%. According to Table 1, the contents of Ti deviate from the nominal composition stoichiometry in 20Cu and 16Cu alloys, while it is very close to the stoichiometry in 10Cu alloy. This seems to explain the absence of the third peak in the latter alloy. A somewhat similar hysteresis behavior at 100 K was observed by Biscarini et al. [18] in the elastic constant measurement for the $Ti_{50}Ni_{30}Cu_{20}$ alloy, and it was interpreted as due to the second B19–B19′ transformation. Obviously the interpretation is different from ours described above. More work is required to clarify the nature of the third peak.

From the step-cooling and step-heating curves in Fig. 3(a) and (b), we find that a small hysteresis (about 4 K as indicted by arrows) also exists on the higher temperature side of the broad peak, while that on the low-temperature side is negligibly small. This temperature hysteresis even occurs when the equilibrium time is extended to 10 min for each measuring temperature. No transformation is expected in the temperature range of the broad peak for $Ti_{50}Ni_{30}Cu_{20}$ alloy, while the hysteresis in $Ti_{50}Ni_{34}Cu_{16}$ case (Fig. 3(b)) can be attributed to overlapping of second transformation. So it is very strange to observe such a hysteresis in both alloys. The origin of this small hysteresis is not understood yet, because hysteresis is not expected for a purely relaxation peak.

3.3. Importance of the presence of twin boundaries for the broad peak in IF

We emphasized the importance of twin boundaries in martensite for the appearance of the broad peak in our previous work [2]. We now show the direct evidence to prove it by using a single crystal of $Ti_{50}Ni_{30}Cu_{20}$ alloy. One of the advantages of the DMA instrument is that we can deform a specimen in various modes. In the present experiment the DMA instrument was used as a small tensile machine as well. Thus a small single crystal of $0.4 \times 0.3 \times 20$ mm^3 was first deformed by 3% under tensile stress at 298 K where the specimen is in the martensitic state, and then unloaded. Since the single crystal was not deformed until the end of the stress–strain plateau, it was not a martensite single crystal, but we can say that the twin boundary density was largely reduced by this process. Thereafter the specimen was cooled directly from 298 K in multi-frequency tension mode with an amplitude of 2 μm. The results are shown in Fig. 4 for $\tan\delta$ (open symbols in

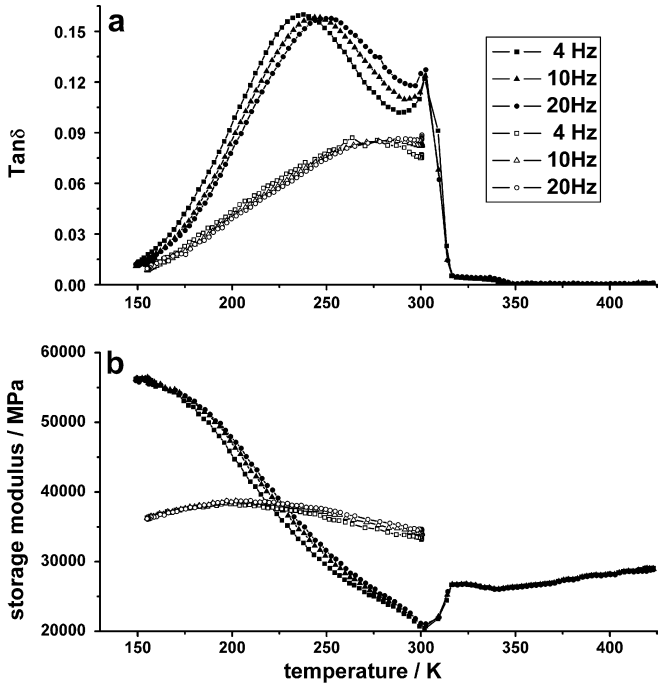

Fig. 4. (a) tan δ and (b) storage modulus as a function of temperature during continuous cooling (2 K/min) for a $Ti_{50}Ni_{30}Cu_{20}$ single crystal at three different frequencies. The open symbols represent the data for the specimen after pre-straining by 3% at 298 K. The filled symbols represent results for the same specimen upon cooling from 423 K after the first experiment described above, where the specimen consists of multi-variants of martensite. The single crystal was solution-treated at 1273 K for 1.5 h, followed by water quenching. See text for details.

Fig. 4(a)) and storage modulus (open symbols in Fig. 4(b)). After these measurements, the specimen was heated to 423 K (in cubic B2 state) and then cooled using the same method but without any pre-strain. The result is shown by filled symbols in Fig. 4(a) and (b). By comparing the two tan δ curves, we clearly see the following. When the specimen is cooled from the cubic state, many twin boundaries are introduced to reduce the total strain energy, and the corresponding tan δ curves show a large broad peak with clear frequency dependence as observed for polycrystal specimens. However, if the specimen is subjected to a prior tensile test in the martensitic state so that the twins are largely eliminated, the broad peak disappears. This directly shows that the presence of twin boundaries is indispensable for the appearance of the broad peak.

3.4. Effect of hydrogen on IF and origin for where H comes from

So far we have described the results for IF behavior of normally heat-treated alloys; i.e. specimens were heat-treated in closed quartz tubes, followed by quenching in water. The specimens were then mechanically polished and chemically etched using a solution consisting of HF:HNO_3:H_2O = 1:4:5. We did not employ an electropolishing method, since electropolishing at low temperature often introduces hydrogen [35]. Thus the method we used will not introduce hydrogen in a normal sense. The important point here is that very high IF is available in the Ti–Ni–Cu alloy system even without hydrogen doping. However, Mazzolai et al. [16–19] claim that IF in Ti–Ni-based alloys is due to hydrogen. So we measured the hydrogen content of our specimens by chemical analysis after DMA measurements, and found that the specimens also contained hydrogen at 0.043 at.%. Although this value is much lower than that reported by others, it is necessary for us to check the effect of hydrogen on the broad peak and also to determine how hydrogen occurs in specimens during normal heat treatment.

Thus, we examined the effect of hydrogen using a vacuum system, as described in Section 2. Fig. 5(a) shows the IF and storage modulus for a $Ti_{50}Ni_{30}Cu_{20}$ specimen,

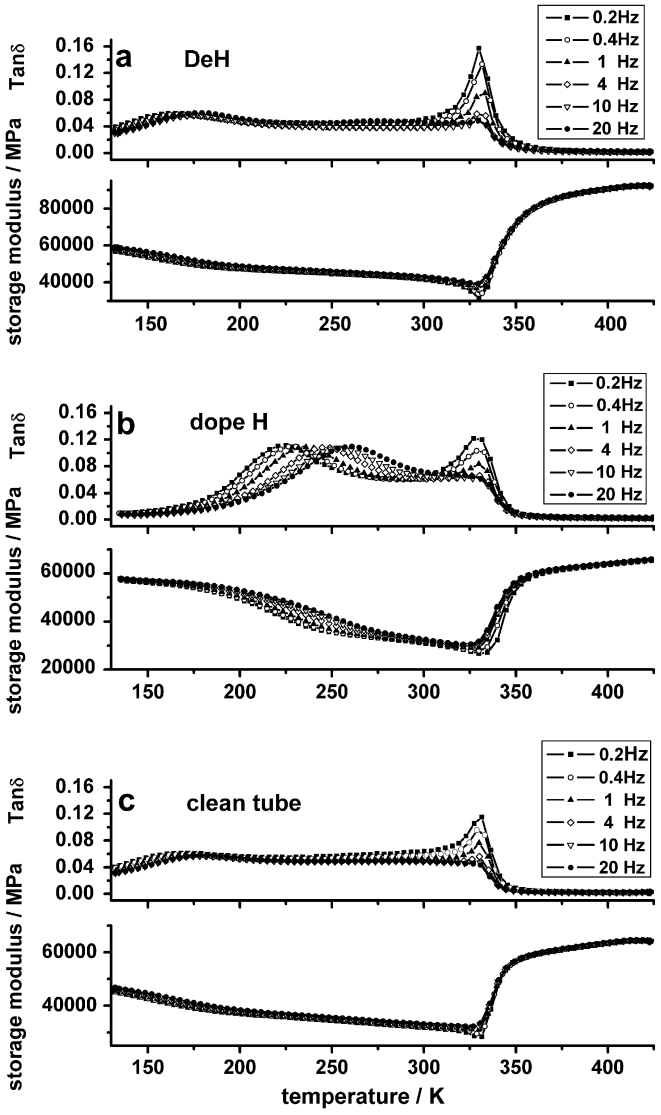

Fig. 5. Internal friction tan δ and storage modulus as a function of temperature during continuous cooling (2 K/min) in DMA multi-frequency strain test mode for $Ti_{50}Ni_{30}Cu_{20}$ specimens after different treatments: (a) DeH at 1173 K for 2 h, (b) keeping in hydrogen atmosphere at 873 K for 1 h after DeH process in (a), and (c) normally solution-treated in a clean closed quartz tube in vacuum without moisture at 1173 K for a fresh $Ti_{50}Ni_{30}Cu_{20}$ specimen. Different symbols represent different frequency as indicated.

which was dehydrogenated by keeping it in a dynamic vacuum at 1173 K for 2 h after normal heat treatment. Compared with Fig. 1(a), the broad peak at 250 K disappears on DeH. Furthermore, when the specimen was doped with hydrogen by keeping it in an H_2-containing closed tube at 873 K, the strong broad peak appeared again near 250 K, as shown in Fig. 5(b). These two experiments clearly show that hydrogen has a strong influence on the broad peak, as Mazzolai et al. claimed, but the implication is different, as we discuss in Section 3.5. Although the 250 K peak disappears after DeH in Fig. 5(a), we still see an IF peak at lower temperature near 180 K. The peak height is very small compared to the 250 K peak in Fig. 5(b). The peak shows a frequency dispersion feature as a relaxation-type peak, the origin of which needs further study. This result is different from those of Mazollai et al. and Sakaguchi et al. [21], who reported that no peak appears without hydrogen doping. Although the reason for the difference between the present results and the previous results is not known, there are some differences in the experimental conditions. Firstly, the testing amplitude is orders of magnitude different. We measured our specimens under a surface strain of 10^{-4}, while Mazzolai et al. carried out experiments at 10^{-6}. Secondly, the frequency range was different: Mazzolai et al. used values of the order of kHz mostly, while we used values of the order of Hz. Thirdly, Sakaguchi et al. used a different method (Ti–Ni/Cu laminated method) to make alloys, and the composition was different. Additionally, we mention here that the peak height of the transition peak for the B2–B19 transformation in Fig. 5 is much higher than that in Fig. 1. This is because the results in Fig. 5 were obtained with continuous cooling with a rate of 2 K/min, while those in Fig. 1 were obtained by step-cooling.

The experiments discussed above show that a small amount of hydrogen somehow getting into the specimens during specimen treatment has a great influence on the occurrence of quite a high broad peak (the 250 K peak). Thus the next problem is to find out how hydrogen gets into the samples during normal heat treatment, since hydrogen is not doped in the present experiments except those of Fig. 5(b). We considered various possibilities such as chemical etching, water quenching, etc., by carrying out DMA measurements under various conditions. However, these were confirmed not to be the main cause, e.g. the broad peak appears even without etching, although etching can increase the height of the broad peak a little. Similarly breaking the tube or not upon quenching did not affect the broad peak appreciably. Thus we supposed that hydrogen is introduced during solution treatment from residual moisture, which was adsorbed on the inner surface of the quartz tubes, by the following chemical reactions:

$$\mathrm{TiNi} + \mathrm{H_2O} \rightarrow \mathrm{TiNi(O)_{soln}} + \mathrm{H_2} \quad (2)$$

or

$$\mathrm{TiNi} + 2\mathrm{H_2O} \rightarrow \mathrm{TiO_2} + \mathrm{Ni} + 2\mathrm{H_2} \quad (3)$$

In Eq. (2), $\mathrm{TiNi(O)_{soln}}$ means that, within the solid solubility range, oxygen is incorporated into TiNi specimens as a solid solution (probably occupying the interstitial sites). When the oxygen content exceeds the solid solubility limit, the reaction accompanies an enrichment of Ni according to Eq. (3), which is supported by our recent studies [36]. This idea explains well the disappearance of the broad peak at 250 K by the solution treatment in a dynamic vacuum described above. If the idea is correct, we expect that the broad peak will be similar with the DeH one, when we use a clean tube without any moisture for solution treatment. To test this, we prepared a clean tube by heating a quartz tube in a dynamic vacuum by H–O firing before fusing the quartz tube for a $Ti_{50}Ni_{30}Cu_{20}$ specimen. After the solution treatment using such a clean tube, DMA measurements were carried out without chemical etching, and the result is shown in Fig. 5(c). We see that the broad peak at 250 K disappeared and a small peak appeared at the same temperature as the DeH case shown in Fig. 5(a). A more systematic study has been carried out for Ti–Ni binary alloys and the result will be published in a future paper [37]. Furthermore, we carried out an experiment to investigate reaction (2) directly by using D_2O instead of H_2O. We detected D_2 with a mass spectrometer as a result of the above reaction, as will also be reported in a future paper [37]. Thus it would be reasonable to conclude that hydrogen is introduced as a result of reaction (2) between the remaining H_2O and Ti at high temperature during solution treatment, and the hydrogen enters the specimens upon cooling.

From the above we can summarize that the presence of a high density of twin boundaries and hydrogen are two key factors for the appearance of a high broad peak in the IF curves for Ti–Ni–Cu alloys.

3.5. Some considerations on the origin of the broad peak

In this section, we discuss briefly the origin of the broad peak. Mazzolai et al. claim that it originates from the stress-induced diffusion of hydrogen, similar to the Snoek peak in body-centered cubic crystals [19], although they also suggested the dragging process of hydrogen by twin boundaries in another paper [17]. However, the broad peak occurs in the B19 martensitic phase, which is a close-packed structure rather than an open one as the B2 structure in the present case. Sakaguchi et al. [21] suggested it to be the Snoek–Koester peak, which results from dislocation movement controlled by the diffusion of segregated interstitial atoms. If the existing dislocations are the reason for the peak, we expect the peak height to increase with dislocation density. However, Zhu et al. [23] found that the peak height decreased by thermal cycling due to the dislocations introduced during martensitic transformation.

Meanwhile, the activation energies associated with the broad peak were obtained as: 0.67 eV for $Ti_{50}Ni_{30}Cu_{20}$, and 0.76 eV for $Ti_{50}Ni_{34}Cu_{16}$. These values look rather too high for the diffusion of hydrogen as in the Snoek peak.

Lord [38] reported the activation energy of 0.13 eV for the hydrogen Snoek peak in Fe, and Canneli and Verdini [39] reported the activation energy of 0.12 eV for the hydrogen Snoek peak in Ta and Nb. Obviously the host crystal is different, and thus the activation energy may be different from that of Ti–Ni–Cu, but the difference seems to be too large. Considering this and the fact that the broad peak appears in the martensitic phase, which has a close-packed structure, it is unlikely that the broad peak is a Snoek peak due to simple hydrogen diffusion under stress.

The results discussed in Sections 3.3 and 3.4 clearly show that both twin boundaries and hydrogen are necessary to observe the broad peak at 250 K. This indicates that the broad peak originates from the interaction of hydrogen with the twin boundaries, and the high value of the activation energy excludes the simple mechanism of hydrogen diffusion. The Snoek–Koester mechanism speculated by Sakaguchi et al. is similar in this regard. However, we do not think it appropriate to treat the twin boundaries as consisting of parallel line dislocations, since twinning shear in martensite often (including the present case) has irrational Burgers vectors. We will have to wait for more detailed mechanisms in this regard. Thus, although there are some differences in the details among Mazzolai's group, Sakaguchi et al. and us, it may be summarized in a broad sense such that the broad peak originates from the interaction of hydrogen with twin boundaries. Concerning the low-temperature relaxation peak[1] newly found around 178 K, we consider it originates from the intrinsic twin boundary motion per se, because it appears in the DeH state. However, to understand the mechanism of this small relaxation peak further detailed studies are needed.

We should mention that the 178 K peak here appearing for the DeH specimen is different from the third peak described in Section 3.2. The third peak is characterized by a small hysteresis, while the 178 K peak shows no hysteresis during step-cooling and step-heating, and the frequency dispersion feature indicates it is a relaxation-type peak. Considering why the third peak does not occur for the DeH specimen but does for the normally treated specimen, we can speculate that the third peak may be related to the martensitic transformation of some kind of hydride, probably due to Ti_2(Ni,Cu)–H precipitates. This may explain why Biscarini et al. [18] found a similar peak only in specimens with a certain amount of hydrogen.

4. Conclusions

The IF of $Ti_{50}Ni_{50-x}Cu_x$ ($x = 10, 16, 20$) alloys, which were normally solution-treated in closed quartz tubes followed by quenching into water, were systematically studied as a function of frequency (0.2–20 Hz) and composition using DMA, generally under step-cooling/heating conditions. The effect of twin boundaries and hydrogen on the IF was also studied using single crystals and a vacuum system with a mass spectrometer, respectively. The results are summarized as follows:

(1) Three well-behaved IF peaks were observed for alloys with $x = 16$ and 20. From high to low temperature, the first peak is the transient peak due to the B2–B19 transformation. The second is the broad peak with clear frequency dispersion. The third very small one appearing below the broad peak with temperature hysteresis was tentatively interpreted as due to the martensitic transformation of Ti_2(Ni,Cu)–H precipitates.

(2) The broad peak at 250 K was confirmed to be a relaxation peak occurring in B19 martensite with the following activation energy (E) and time constant (τ_0): $Ti_{50}Ni_{30}Cu_{20}$, $E = 0.67 \pm 0.01$ eV, $\tau_0 = 2.0 \times 10^{-15\pm0.1}$ s; $Ti_{50}Ni_{34}Cu_{16}$, $E = 0.76 \pm 0.02$ eV, $\tau_0 = 2.1 \times 10^{-17\pm0.4}$ s.

(3) In an experiment using a $Ti_{50}Ni_{30}Cu_{20}$ single crystal, the broad peak was found to disappear by largely eliminating martensite twin boundaries. This is direct evidence to show that the presence of twin boundaries is indispensable to observe the broad peak.

(4) The results show that the present alloys exhibit very high broad peaks even without hydrogen doping (the hydrogen content in normally heat-treated specimens was 0.043 at.% as determined by chemical analysis). However, this peak was confirmed to be related to hydrogen, because it disappears on dehydrogenation in a dynamic vacuum system, and reappears again at the same temperature on hydrogen doping.

(5) Although the broad peak at 250 K disappears on DeH, as stated above, a new relaxation peak was found at 178 K in the DeH condition. This peak was interpreted as a relaxation peak intrinsic to the twin boundary motion per se without hydrogen.

(6) We have shown that hydrogen is introduced in normal heat-treatment by the chemical reaction of residual H_2O in quartz tubes with Ti at high temperature:

$$TiNi + H_2O \rightarrow TiNi(O)_{soln} + H_2$$

or

$$TiNi + 2H_2O \rightarrow TiO_2 + Ni + 2H_2$$

(7) From the above we can summarize that there are two essential ingredients to observe the high broad peak in the present alloys: hydrogen and high-density mobile twin boundaries in martensite. Thus we may suppose the following. The broad peak at 250 K is a relaxation peak, which originates from the interaction of hydrogen with the motion of high-density twin boundaries in martensite, although the detailed mechanism remains to be elucidated.

[1] Although the peak temperature is frequency-dependent, we may take 178 K for 4 Hz as a representative peak temperature for the low-temperature peak, since the broad peak without DeH appears at 250 K for 4 Hz in the present work. Thus we may call it the "178 K peak".

Acknowledgements

The authors are grateful to Prof. F.M. Mazzolai and the late Prof. S. Okuda for useful discussions on the effect of hydrogen on the IF of alloys. They also acknowledge Prof. Yu.I. Chumlyakov for providing $Ti_{50}Ni_{30}Cu_{20}$ single crystals, and Prof. J. Sun for encouragement and stimulating discussions. The present work was supported by the Grant-in-Aid for Scientific Research (Kiban-C) from the Japan Society for the Promotion of Science.

References

[1] Van Humbeeck J. J Alloys Compd 2003;355:58.
[2] Yoshida I, Monma D, Iino K, Otsuka K, Asai M, Tsuzuki H. J Alloys Compd 2003;355:79.
[3] Saburi T. In: Otsuka K, Wayman CM, editors. Shape memory materials. Cambridge: Cambridge University Press; 1998. p. 49.
[4] Otsuka K, Ren X. Prog Mater Sci 2005;50:511.
[5] Nam TH, Saburi T, Shimizu K. Mater Trans JIM 1990;31:959.
[6] Shugo Y, Hasegawa H, Honma T. Bull Res Inst Mineral Dressing Metall, Tohoku Univ 1981;37:79 [in Japanese].
[7] Tadaki T, Wayman CM. Metallography 1982;15:233. 247.
[8] Watanabe Y, Saburi T, Nakagawa Y, Nenno S. J Jpn Inst Met 1990;54:861 [in Japanese].
[9] Nam TH, Saburi T, Nakata Y, Shimizu K. Mater Trans JIM 1990;31:1050.
[10] Fukuda T, Saburi T, Chihara T, Tsuzuki Y. Mater Trans JIM 1995;36:1244.
[11] Miyamoto H, Taniwaki T, Ohba T, Otsuka K, Nishigori S, Kato K. Scripta Mater 2005;53:171.
[12] Ohba T, Taniwaki T, Miyamoto H, Otsuka K, Kato K. Mater Sci Eng A, in press.
[13] Lo YC, Wu SK, Horng HE. Acta Metall Mater 1993;41:747.
[14] Lin HC, Wu SK, Chang YC. Metall Mater Trans 1995;26A:851.
[15] Yoshida I, Monma D, Iino K, Ono T, Otsuka K, Asai M. Mater Sci Eng A 2004;370:444.
[16] Coluzzi B, Biscarini A, Campanella R, Trotta L, Mazzolai G, Tuissi A, et al. Acta Mater 1999;47:1965.
[17] Mazzolai FM, Biscarini A, Campanella R, Coluzzi B, Mazzolai G, Rotini A, et al. Acta Mater 2003;51:573.
[18] Biscarini A, Coluzzi B, Mazzolai G, Mazzolai FM, Tuissi A. J Alloys Compd 2003;356–357:669.
[19] Mazzolai FM, Coluzzi B, Mazzolai G, Biscarini A. Appl Phys Lett 2004;85:2756.
[20] Igata N, Urahashi N, Sasaki M, Kogo Y. J Alloys Compd 2003;355:85.
[21] Sakaguchi T, Uehara T, Kogo Y, Takeuchi S, Igata N. Mater Trans 2005;46:1306.
[22] Hasiguti RR, Iwasaki K. J Appl Phys 1968;39:2182.
[23] Zhu JS, Schaller R, Benoit W. Phys Lett 1989;141:177.
[24] Yoshida I, Yoshida S. Solid State Phenom 2003;89:315.
[25] Snoek JL. Physica 1941;8:711.
[26] Koester W, Bangert L, Hahn R. Arch Eisenhutterw 1954;25: 569.
[27] Aoyagi T, Sumino K. Phys Status Solidi 1969;33:317.
[28] Yin F, Nagai K, Watanabe K, Kawahara K. Mater Trans 2003;44:1671.
[29] Murakami Y, Otsuka K, Mizubayashi H, Suzuki T. In: Inoue K, Mukherjee K, Otsuka K, Chen H, editors. Displacive phase transformations and their applications in materials engineering. Warrendale (PA): TMS; 1998. p. 225.
[30] Shen HM, Huang YN, Zhang ZF, Yang Z, Wang XM, Wang YN, et al. Mat Res Soc Symp Proc 1996;398:513.
[31] Huang YN, Ding YN, Wang YN, Shen HM, Zhang ZF. Phys Rev 1997;55B:16159.
[32] Nowick AS, Berry BS. Anelastic relaxation in crystalline solids. New York (NY): Academic Press; 1972. p. 52.
[33] Hara T, Ohba T, Otsuka K, Nishida M. Mater Trans 1997;38:277.
[34] Golberg D, Otsuka K. Unpublished work, 2005.
[35] Nishida M, Yamauchi K, Chiba A, Higashi Y. In: Proceeding of the ICOMAT-92, Monterey, Monterey Institute for Advanced Studies, 1993. p. 881.
[36] Zhang J. to be submitted for publication.
[37] Fan G et al. to be submitted for publication.
[38] Lord AE. Acta Metall 1967;15:1241.
[39] Cannelli G, Verdini L. Ric Sci 1966;36:98.